Cotransport-Induced Instability of Membrane Voltage in Tip-Growing Cells

M. Leonetti, P. Marcq, and J. Nuebler
IRPHE, Universités Aix-Marseille I and II, UMR CNRS 6594, Technopôle de Château-Gombert, 13384 Marseille Cedex 13, France

F. Homble
Laboratory for Structure and Function of Biological Membranes, Université Libre de Bruxelles, CP206/2, Campus Plaine, B-1050 Brussels, Belgium
(Received 24 May 2005; published 10 November 2005)

A salient feature of stationary patterns in tip-growing cells is the key role played by the symports and antiports, membrane proteins that translocate two ionic species at the same time. It is shown that these cotransporters destabilize generically the membrane voltage if the two translocated ions diffuse differently and carry a charge of opposite (same) sign for symports (antiports). The orders of magnitude obtained for the time and length scale are in agreement with experiments. A weakly nonlinear analysis characterizes the bifurcation.

DOI: 10.1103/PhysRevLett.95.208105 PACS numbers: 87.10.+e, 05.65.+b, 87.16.Uv

Spatiotemporal pattern formation of the electric membrane potential in cells and tissues emerges from collective dynamics and activity of membrane ion channels. Action potential and cardiac excitation spiral waves are paradigmatic examples of nonstationary pattern formation [1,2]. Stationary patterns of ionic currents are widespread in fungi, plant cells (algae, for example), protozoa, and insects: Chara corallina, Fucus zygote, and Achlya are the model cells [3,4]. Such patterns are correlated to cell polarization, apical growth, morphogenesis, and nutrient acquisition. The characteristic wavelengths and times vary from a few millimeters to 10 μm and from 1 h to 1 min, respectively. These times correspond typically to a membrane protein or an ion diffusive time. Two mechanisms have been proposed [5]: one based on the electromigration of membrane proteins [6–10] and the other resulting from a negative differential conductance characterizing voltage-gated channels [11–13].

However, the origin of current patterns is still unclear in tip-growing cells where transcellular currents are mainly produced by the pump and a cotransporter, a membrane carrier that translocates two species of ions at the same time [14,15] (see Fig. 1). Three points of view are proposed by biologists for tip-growing cells: ionic currents may be a consequence of cellular growth, a self-organized pattern coupled to growth, or, alternatively, arise as a self-organized pattern which precedes cellular growth [16]. The appearance of a lateral branching preceded by an inward current supports the hypothesis of self-organization in Achlya [15]. The mechanisms proposed in the literature cannot explain such patterns [17].

In this Letter, we ask the broader question: How does the stability of the membrane voltage depend on cotransporters? Only the contribution of channels to membrane voltage instability has been investigated in the literature. We demonstrate here that the voltage along a membrane containing cotransporters is linearly unstable on a diffusive (not electrical) characteristic time. The final pattern is a stationary modulation of ionic concentrations, membrane voltage, and transcellular ionic currents. The mechanism is specific to this kind of carrier since each ionic transporter is characterized by a *positive* differential conductance.

Consider two ions 1, 2 of valence numbers z_j and concentrations C_j, diffusing along a cylindrical cellular membrane of radius r. As in the cable model, the electrodynamics is governed by a one-dimensional electrodiffusive equation for each ion,

$$\partial_t C_j = D_j \partial_x^2 C_j + z_j (e D_j / k_B T) \partial_x (C_j \partial_x V) - (2/r) J_j, \quad (1)$$

and the capacitive relation for the membrane voltage V,

$$V = V_0 + (Fr/2C_m)[z_1(C_1 - C_{10}) + z_2(C_2 - C_{20})], \quad (2)$$

where D_j is the diffusion coefficient of ion j, V_0 the resting membrane potential (≈ -0.1 V), C_m the specific membrane capacitance (≈ 0.01 F m^{-2}), and C_{j0} the concentration of ion j in the resting state. The standard cable model is recovered simply from (1) and (2) when all ionic diffu-

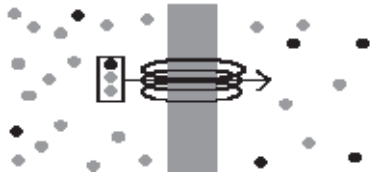

FIG. 1. The pump (not drawn) generates a gradient of the electrochemical potential through the membrane by translocating continuously one species of ions (gray disk). This stored free energy is used by the symport, a cotransporter, to transfer a second species of ion (black disk) or nutrient against its own gradient if necessary. The stoicheiometry of the drawn symport is equal to 2: two gray disks for one black disk.

sion coefficients are identical. In our model, the fluxes J_j take into account the intracellular chemical reactions as well as the membrane fluxes through pumps, cotransporters, channels, and uniports. The pump uses chemical energy [adenosine triphosphate (ATP)] to translocate ions from one side to the other (the 1-ion in this Letter), generating an electrochemical potential gradient through the membrane: for example, H^+-ATPase in plant cells. Consequently, the 1-ion is a cation. Cotransporters use this stored free molar energy to transfer one 2-ion for n 1-ions in the same (opposite) sense for the symport (antiport) carrier (see Fig. 1). In practice, the stoicheiometry n is equal to either 1 or 2. In tip-growing cells, the 2-ion is often an essential nutrient for future vegetal metabolism and consequently, implied in many chemical processes based on enzymatic binding reactions, metabolism in Achlya hyphae with the methionine (an amino acid) uptake or the carbon dioxide supply to chloroplasts for photosynthesis in Chara corallina by HCO_3^- entry. Finally, the flux J_j of each ion j is

$$J_1 = J_{\text{pch}} + nJ_s, \tag{3}$$

$$J_2 = \pm J_s + \alpha C_2 + J_2^{\text{NL}}, \tag{4}$$

where J_{pch} is the flux through active pumps and passive channels translocating the 1-ion, $\pm J_s$ (nJ_s) is the flux of the 2-ion (1-ion) through the cotransporter, and J_2^{NL} is the (concentration-dependent) nonlinear part of J_2, due to intracellular chemical processes. The mechanism of the (linear) voltage instability does not depend on the functional form of J_2^{NL}. The characteristic kinetic constant α of nutrient uptake is necessarily positive. The sign $\pm$ is $+$ for a symport and $-$ for an antiport. In the following, we consider the case of the symport but the extension to that of the antiport is straightforward. For simplicity's sake, J_{pch} and J_s do not depend on concentrations and vary linearly with the membrane potential V, characterized by their positive conductances: $G_{\text{pch}} = z_1F(\partial J_{\text{pch}}/\partial V)$ and $G_s = z_1F(\partial J_s/\partial V)$. Even if a cotransporter is often called a secondary active carrier, its working is passive. Consequently, the differential conductance of the current through the cotransporter, $(n + z_2/z_1)G_s$ is always positive (positive Onsager coefficient). Then, there is no local positive feedback provided by protein characteristics. In the homogeneous resting state, $J_j = 0$ for each ion: the molar flux J_{s0} of the nutrient uptake in the resting state may be nonzero. Equations (1)–(4) are scaled with dimensionless coordinates for space $x' = x/\lambda$ and time $t' = t/\tau$ with the cable length characteristic of the pumps and channels (primes are then dropped for simplicity), $\lambda^2 = r\gamma/2G_{\text{pch}}$, and the diffusive time $\tau = \tilde{D}\lambda^2/D_1D_2$, where γ is the bulk ionic conductivity and $\tilde{D} = \delta_1D_1 + \delta_2D_2$ is the mean coefficient of diffusion. We set $\delta_j = z_j^2C_{j0}/(z_1^2C_{10} + z_2^2C_{20})$ equal to 0.5 in all the following.

The control parameter μ is the positive conductance ratio, $\mu = G_s/G_{\text{pch}}$, that controls the ionic membrane fluxes. The stability of the homogeneous equilibrium state is analyzed by considering the evolution of fluctuations of voltage V and ionic concentrations C_j and consequently the linearized equations of (1)–(4): $\delta H(x, t) = \delta H_0 e^{st+ikx}$, where k is the wave number of the perturbation and H refers to V and C_j. Two real solutions for $s = s(k)$ are determined: $\text{Im}(s) = 0$, $\text{Re}(s) = \sigma(\mu; k)$. The first one is the well-known fast capacitive relaxation. The second one yields the growth rate of the instability:

$$\sigma(\mu; k) = -\frac{k^4 + \frac{\tilde{D}}{D_1}k^2[1 + \mu(n + \frac{D_1z_2}{D_2z_1})]}{k^2 + 1 + (n + z_2/z_1)\mu} - \frac{\beta_1}{D_2} \times \frac{(\tilde{D} - D_2)k^2 + (D_1 - D_2)(1 + n\mu)\frac{\tilde{D}}{D_1}}{k^2 + 1 + (n + z_2/z_1)\mu}, \tag{5}$$

where $\beta_1 = \alpha\gamma/G_{\text{pch}}(D_1 - D_2)$ is dimensionless. Since the capacitance does not appear in (5), this characteristic (inverse) time is *diffusive*. From $\sigma(\mu_0(k); k) = 0$, the neutral curve $\mu_0(k)$ is determined and has a minimum defining the critical values of the control parameter μ_c and the wave number k_c (Fig. 2):

$$\mu_c = \frac{-D_1D_2}{\tilde{D}(z_2D_1/z_1 + nD_2)}\left[2k_c^2 + \frac{\tilde{D}}{D_1} + \beta_1\left(\frac{\tilde{D}}{D_2} - 1\right)\right],$$

$$(k_c^2 - k_0^2)^2 = k_0^4 + \frac{\beta_1\tilde{D}}{D_1D_2}(D_1 - D_2) + k_0^2\left[\frac{\tilde{D}}{D_1} + \beta_1\left(\frac{\tilde{D}}{D_2} - 1\right)\right],$$

where $k_0^2 = -n\beta_1(D_1 - D_2)/(z_2D_1/z_1 + nD_2)$. The particular case $\alpha = \beta_1 = 0$ corresponds to a long-wavelength instability ($k_c = 0$), and will not be treated here [9].

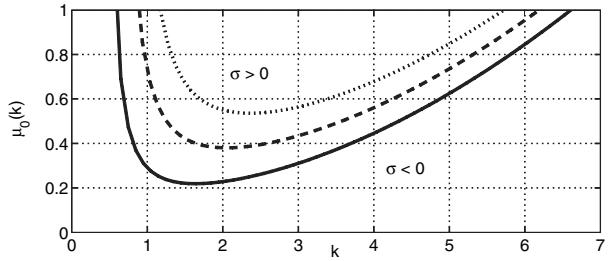

FIG. 2. The neutral curve $\mu_0(k)$ is defined by $\sigma(\mu_0(k); k) = 0$ and has a minimum at $(k_c; \mu_c)$. Above the critical control parameter μ_c, the membrane voltage is unstable. Parameters are $n = 2$, $z_1 = 1$, $z_2 = -1$, $D_1 = 10^{-5}$ cm^2 s^{-1}, $D_2 = 10^{-7}$ cm^2 s^{-1} (common for the three neutral curves), and $\beta_1 = 0.1$ (solid line), $\beta_1 = 0.2$ (dashed line), and $\beta_1 = 0.3$ (dotted line).

For $\mu > \mu_c > 0$, the growth rate is positive in a finite range of wave numbers. The limit case of small binding reactions may help clarify the nature of this instability. For small but nonzero β_1, the homogeneous resting state is unstable ($\sigma > 0$) against spatial perturbations if $1 + \mu(n + D_1 z_2/D_2 z_1) < 0$. Recalling that $0 \leq n + z_2/z_1$, two necessary conditions for instability are $D_1 > nD_2|z_1/z_2|$ and $z_2/z_1 < 0$ [18]. The former is generally verified since binding reactions reduce notably the effective diffusion of the 2-ion [19]; the latter is fulfilled for the symports H^+/HCO_3^- in Chara corallina and H^+-methionine in Achlya. For large control parameter μ and small β_1, the wavelength λ_p of the pattern satisfies: $\lambda_p \approx 2\pi(r\gamma D_2/2G_s\tilde{D})^{1/2} \approx \lambda_{\text{cable}}(D_2/\tilde{D})^{1/2}$, where λ_{cable} is provided by the cable model and may be experimentally measured by two impaled electrodes. An order of magnitude of λ_p can thus be evaluated. In Achlya hyphae, some measurements indicate $\lambda_{\text{cable}} \approx 2$ mm [20]. On the basis of measurements of the effective diffusion of the calcium ion, a reasonable value for the diffusion coefficient of the 2-ion is $D_2 \approx 10^{-7}$ cm^2/s. We thus expect a characteristic pattern wavelength $\lambda_p \approx 100$ μm, in agreement with experiments. The characteristic time τ_p required to produce the pattern is of the order of a diffusive time: $\tau_p \approx \lambda_p^2/D_2$, dominated by the slower ionic diffusion. Using the previous values, we find $\tau_p \approx 10^3$ s, in agreement with experiments on Achlya hyphae [3].

Equations (1)–(4) have been solved numerically for a large range of parameters to confirm the previous results. For simplicity, the nonlinear flux J_2^{NL} is given by a truncated expansion in powers of the concentration of the 2-ion:

$$J_2^{\text{NL}} = C_{20} \sum_{j=2,3} \alpha_j [(C_2 - C_{20})/C_{20}]^j. \tag{6}$$

This form generalizes the expansion of a Michaelis-Menten enzyme kinetics term in the limit of large Michaelis constant: our goal is to take into account at a phenomenological level some of the complexity due to the function of the 2-ion. The coefficient α_3 must be positive to ensure nonlinear convergence. The simulation depends on two additional dimensionless parameters: $\beta_2 = \gamma^2|V_0|\alpha_2/[z_2 F G_{\text{pch}} C_{20}(D_1 - D_2)^2]$ and $\beta_3 = \gamma^3|V_0|^2\alpha_3/[(z_2F)^2 G_{\text{pch}} C_{20}^2(D_1 - D_2)^3]$. Generally, the voltage relaxes to zero on a characteristic capacitive time, as expected from the cable model. However, for relevant parameters characterizing a symport, a cellular pattern of voltage and concentrations appears after a transient whose duration is of the order of magnitude of the diffusive time τ_p (Fig. 3). Outer and inner transcellular currents flow periodically through the membrane. It has been established that the Ohmic part I_{Ohm} of the dimensionless extracellular current normal to the membrane is given by the following relation: $I_{\text{Ohm}} = \tilde{D}(I_1/D_1 + I_2/D_2)/G_{\text{pch}}|V_0|$ [12]. An outer (inner) ohmic current corresponds to an hyperpolarized (depolarized) band in agreement with experiments (Fig. 3). The outer current has a characteristic M shape, observed in Chara corallina. Varying the nonlinear parameters, it is possible to obtain a M shape only for the inner current or for both.

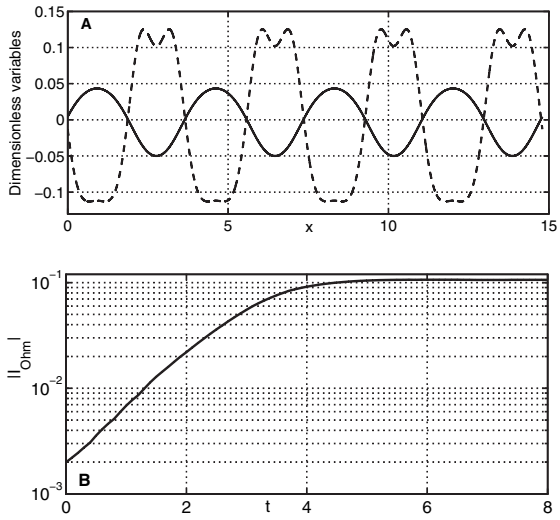

FIG. 3. Parameters are the same as in Fig. 2, with additional $\mu = 0.25$, $\beta_1 = 0.1$, $\beta_2 = 0.1$, and $\beta_3 = 5$. (a) The final stationary pattern is a modulation of the dimensionless membrane potential $(V - V_0)/|V_0|$ (solid line) and of the dimensionless Ohmic part I_{Ohm} (dashed line) of the extracellular current. An hyperpolarized membrane potential $(V - V_0)/|V_0| < 0$ corresponds to an outer Ohmic current (electric field) in agreement with experiments made with the vibrating probe. (b) Temporal evolution of the extracellular current I_{Ohm} at the position $x = 12.5$. The characteristic time is an ionic diffusive one.

The stationary bifurcation is further characterized by a weakly nonlinear analysis performed in the vicinity of the threshold $(k_c; \mu_c)$ [2]. An arbitrarily small expansion parameter ϵ is introduced to separate the fast and slow scales in the problem. We define the slow independent variables $X = \epsilon x$ and $T = \epsilon^2 t$, and Taylor expand the concentrations C_j, membrane voltage V, and control parameter μ in powers of ϵ. The resulting equations are then solved recursively for each power ϵ^i. The solvability condition (Fredholm alternative) at third order provides the amplitude equation:

$$\tau_0 \partial_T A = \bar{\mu} A + \xi_0^2 \partial_X^2 A - g|A|^2 A, \tag{7}$$

where $\bar{\mu} = (\mu - \mu_c)/\mu_c$ is the reduced control parameter. The time and length scale τ_0 and ξ_0 of the pattern's slow modulations close to the bifurcation may also be derived directly from the dispersion relation (5): $\mu_c \xi_0^2 = \frac{1}{2}(\partial^2 \mu_0/\partial k^2)_c$ and $\tau_0^{-1} = \mu_c(\partial\sigma/\partial\mu)_c$ [2]. The coefficient g of the nonlinear term is a complicated function of the physical parameters. The bifurcation is supercritical (subcritical) for positive (negative) values of g. In the

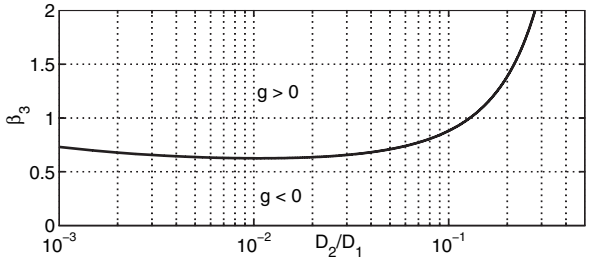

FIG. 4. The tricritical line $g = 0$ separates domains in the reduced parameter space $(D_2/D_1; \beta_3)$ where the bifurcation is supercritical ($g > 0$) and subcritical ($g < 0$). The fixed parameter values are the same as in Fig. 3.

idealized case described here, and for typical parameter values, a tricritical line $g = 0$ separates the two types of bifurcation in parameter space (see Fig. 4).

In conclusion, we established that a spatially homogeneous membrane voltage is linearly unstable if the cotransporters play a role in the control of the electrophysiological properties of a cell. The final stationary pattern is a transcellular current bearing various ionic species. As opposed to many other scenarios leading to spatiotemporal pattern formation in ionic currents [1,11,12], a negative differential conductance is not required. A necessary ingredient is the slow intracellular diffusion of one of the two ions translocated by the cotransporter. Interestingly, this is often the case in experiments. This mechanism may explain how a cell can uptake an essential nutrient at precise locations: in Achlya, methionine enters at the tip during apical growth.

We thank P. Pelcé for useful discussions. We wish to acknowledge the support of "ACI Physico-chimie des systèmes complexes" (France), the Fonds National de la Recherche Scientifique (Belgium), and the Communauté Française de Belgique-Action de Recherches Concertées (Belgium).

[1] For a review, see Special issue on Fibrillation in normal ventricular myocardium, edited by A. T. Winfree [Chaos **8**, 1 (1998)].
[2] M. C. Cross and P. C. Hohenberg, Rev. Mod. Phys. **65**, 851 (1993).
[3] N. A. R. Gow, Adv. Microb. Physiol. **30**, 89 (1989).
[4] For numerous examples of patterns of transcellular currents and a large bibliography, see www.mbl.edu/labs/BioCurrents/Databases.html.
[5] Pattern formation of transcellular ionic currents could also result from a Turing instability. However, contrary to the two other mechanisms, experimental evidence is still lacking.
[6] P. Fromherz and W. Zimmermann, Phys. Rev. E **51**, R1659 (1995).
[7] P. Fromherz, Proc. Natl. Acad. Sci. U.S.A. **85**, 6353 (1988).
[8] M. Leonetti and E. Dubois-Violette, Phys. Rev. E **56**, 4521 (1997).
[9] S. C. Kramer and R. Kree, Phys. Rev. E **65**, 051920 (2002).
[10] Experiments on the effect of electric fields on clustering of acetylcholine receptors proves the relevance of the Fromherz mechanism at scales less than 50 μm. However, the large characteristic time predicted for patterns of larger wavelengths, such as observed in Chara corallina, is not consistent with experiments.
[11] M. Leonetti and E. Dubois-Violette, Phys. Rev. Lett. **81**, 1977 (1998).
[12] M. Leonetti, E. Dubois-Violette, and F. Homble, Proc. Natl. Acad. Sci. U.S.A. **101**, 10 243 (2004), and reference therein.
[13] Contrary to excitable cells such as neurons and cardiac cells, a mismatch between the diffusive properties of the relevant ions inhibits (in a domain of parameters) the electrical instability at the origin of action potential and drives a diffusive linear instability.
[14] L. Limozin, B. Denet, and P. Pelce, Phys. Rev. Lett. **78**, 4881 (1997).
[15] D. L. Kropf, M. D. A. Lupa, J. H. Caldwell, and F. M. Harold, Science **220**, 1385 (1983).
[16] F. M. Harold, in *Tip Growth in Plant and Fungal Cells*, edited by I. B. Heath (Academic Press, San Diego, 1990), p. 59.
[17] As opposed to [11,12], voltage-gated channels are *not* involved here. See also [10].
[18] For antiports, $n + D_1 z_2/D_2 z_1 < 0$ is replaced by $n - D_1 z_2/D_2 z_1 < 0$. The two necessary conditions are $D_1 > nD_2|\frac{z_1}{z_2}|$ (unchanged) and $z_2/z_1 > 0$ (often fulfilled by antiports).
[19] For example, it is well established that the diffusion constant of the calcium ion is then reduced by at least a factor of 100.
[20] D. L. Kropf, J. Cell Biol. **102**, 1209 (1986).